Supporting Information

P3-type $K_{0.32}Fe_{0.35}Mn_{0.65}O_2 \cdot 0.39H_2O$: a promising cathode for Na-Ion full batteries

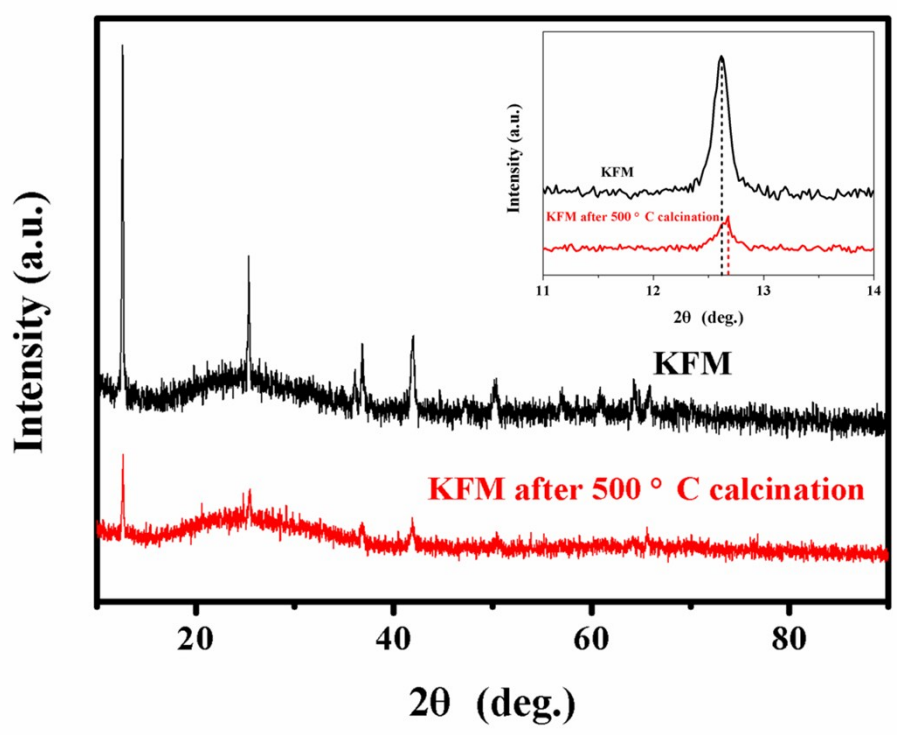

Fig. S1 XRD patterns of the KFM sample and the 500 °C heated KFM sample, the inset shows the details between 11 and 14°. (The heated sample was cooled down in argon-filled glove box and immediately characterized)

Table S1. The calculated lattice reflections, inter-planar distances and peak intensities of KFM by Rietveld refinement.

No.	2θ	h	k	l	D-spacing (Å)	Int. (a.u.)
1	12.618	0	0	-3	7.0097	444697.74
2	25.392	0	0	-6	3.5049	151062.35
3	36.078	-1	1	1	2.4876	178112.72
4	36.854	0	1	2	2.4369	150658.12
5	38.498	0	-9	2	2.3366	19851.07
6	39.828	-1	1	4	2.2615	86947.48
7	41.943	0	1	5	2.1523	205139.9
8	47.202	-1	1	7	1.924	118803.75
9	50.271	0	1	8	1.8135	52785.85
10	52.152	0	0	-12	1.7524	34655.92
11	57.143	-1	1	10	1.6107	40875.84
12	60.909	0	1	11	1.5198	31610.19
13	64.36	-1	2	0	1.4463	45649.45
14	65.886	-1	2	3	1.4165	31699.59
15	66.659	0	0	-15	1.4019	5775.44
16	69.06	-1	1	13	1.3589	23584.97
17	70.36	-1	2	6	1.337	45283.01
18	73.445	0	1	14	1.2883	12791.21
19	76.058	0	2	1	1.2504	15461.18
20	76.533	-2	2	2	1.2438	12659.75
21	77.564	-1	2	9	1.2298	16795.33
22	78.423	0	2	4	1.2185	10189.24
23	79.832	-2	2	5	1.2005	16929.85
24	82.5	0	0	-18	1.1683	4653.22
25	82.882	-1	1	16	1.1639	8224.49
26	83.562	0	2	7	1.1561	13719.24
27	85.879	-2	2	8	1.1308	8536.1
28	87.347	-1	2	12	1.1155	27975.14
29	87.974	0	1	17	1.1092	12451.16

Table S2. Rietveld refinement parameters and results obtained for KFM.

Atoms	x	y	z	Occupancy
K	0	0	0.832921	0.32
Fe	0	0	0	0.35
Mn	0	0	0	0.65
O	0	0	0.409097	1
O	0	0	0.590903	1
$O_{(H2O)}$	0	0	0.832921	0.39

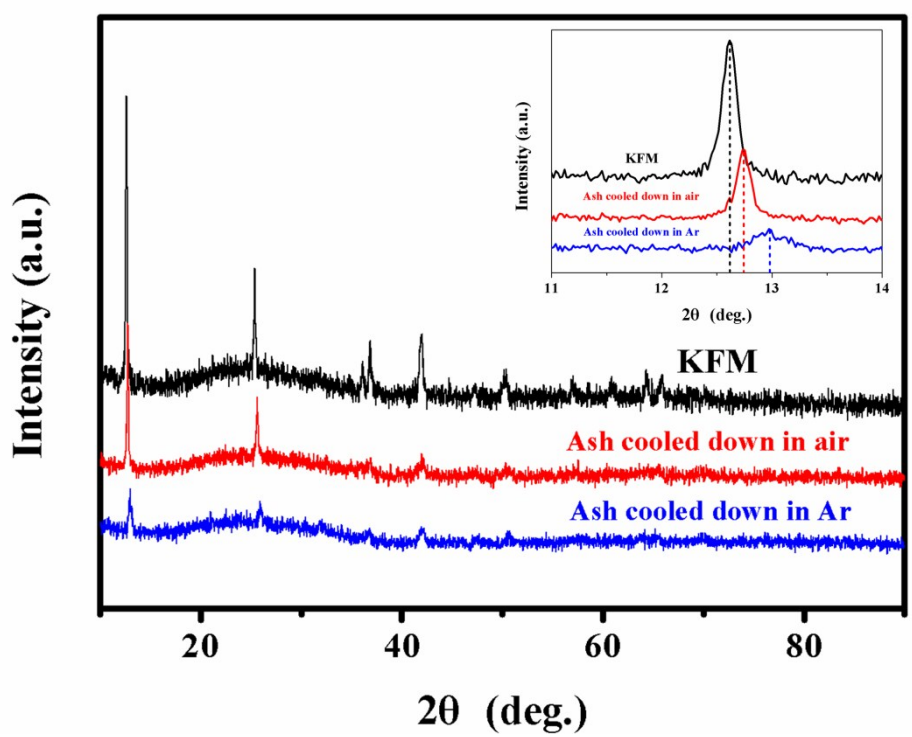

Fig. S2. XRD patterns of the KFM sample and the ash (before the centrifuging step) that cooled down in air and argon-filled glove box, respectively; the inset shows the details between 11 and 14°.

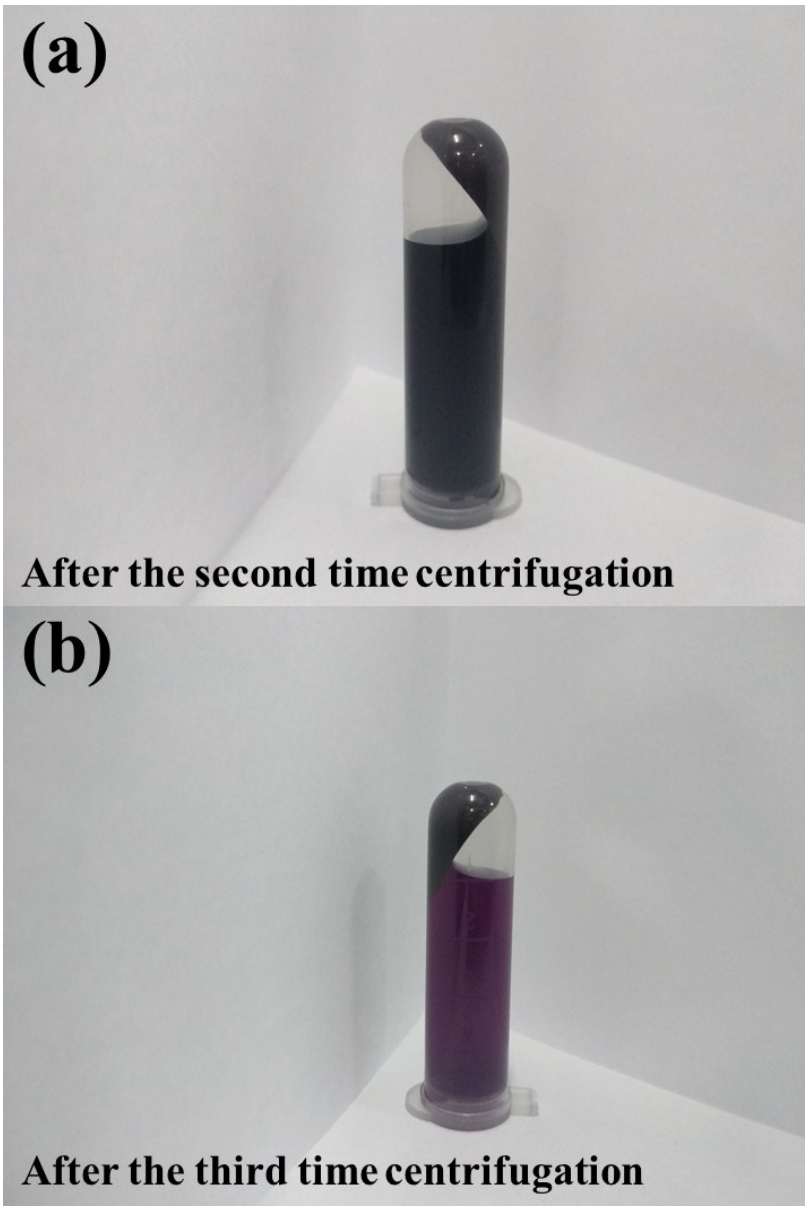

Fig. S3. (a, b) Optical images of the centrifuge tube in the progress of washing the KFM.

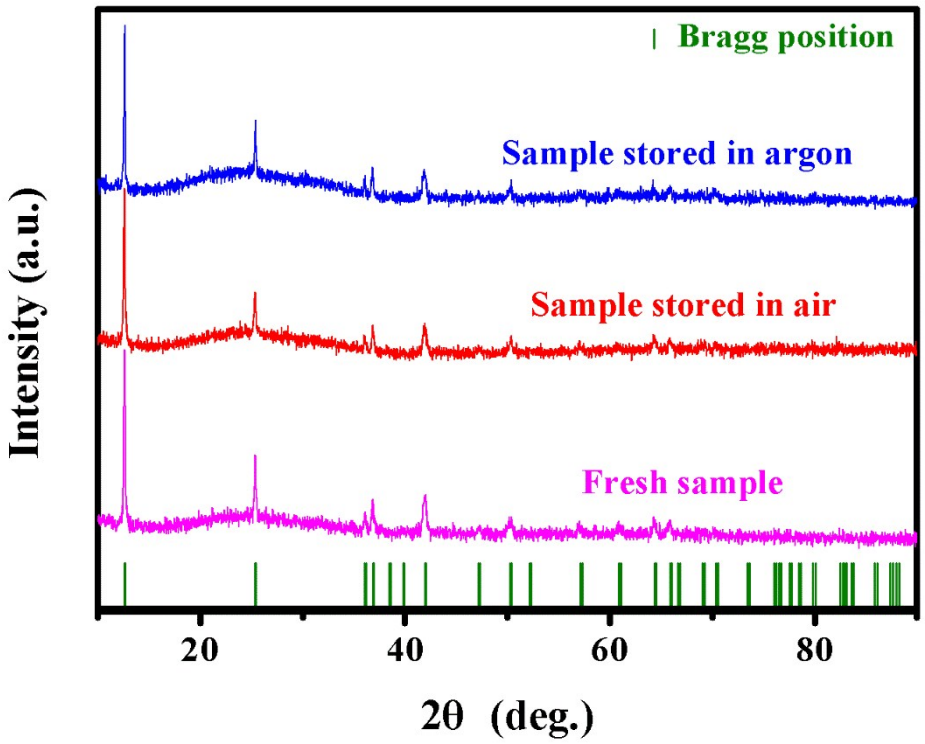

Fig. S4 XRD patterns of the fresh KFM sample and the KFM samples after stored in ambient air and argon (one week).

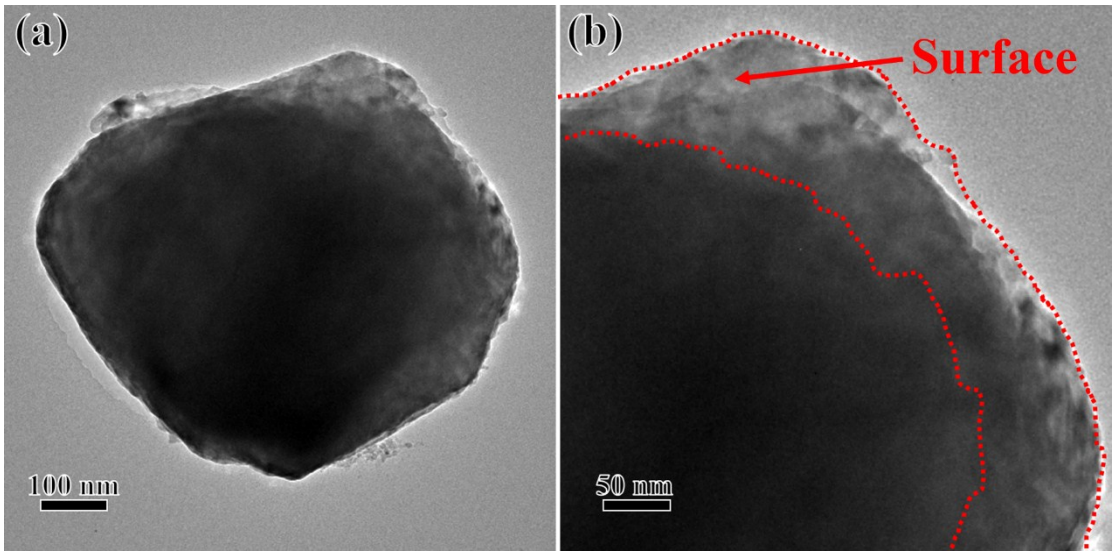

Fig. S5 TEM images of KFM with different magnifications.

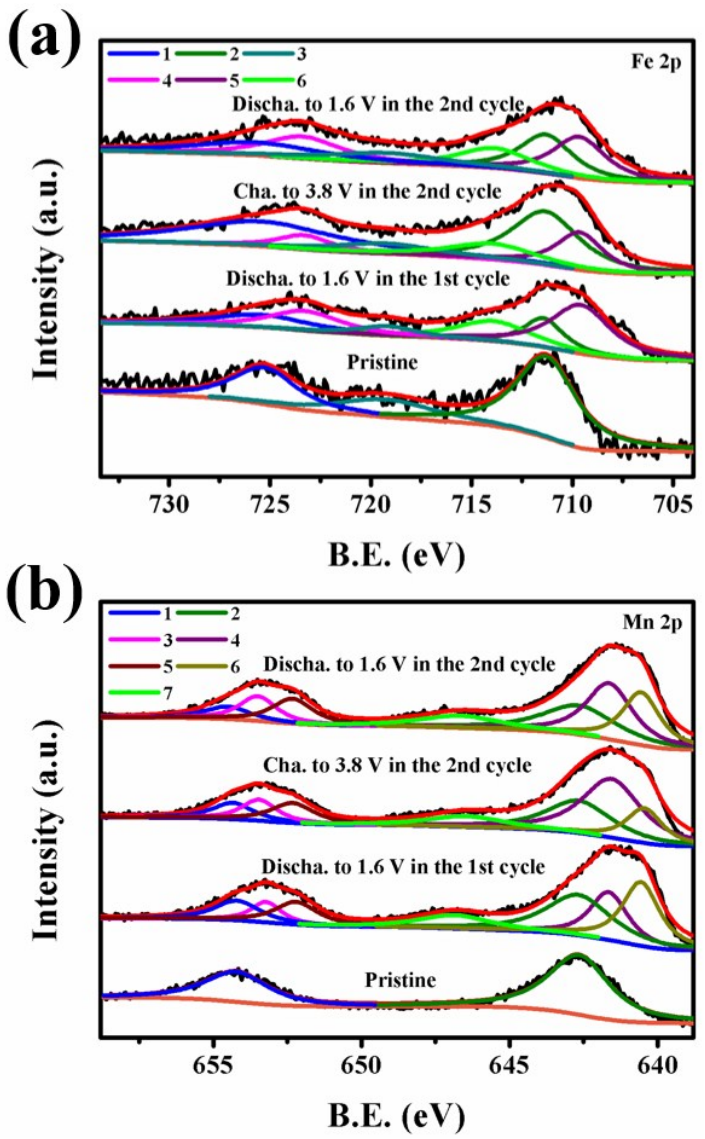

Fig. S6 (a) Fe 2p (Peak 1, 2, 3 for Fe^{3+}, Peak 4, 5, 6 for Fe^{2+}) (b) Mn 2p XPS spectra of KFM in different states during cycling (Peak 1, 2 for Mn^{4+}, Peak 3, 4 for Mn^{3+} and Peak 5, 6,7 for Mn^{2+}).

Ex situ XPS method was employed to further understand the valence change through recording electrodes with different depths of discharge and charge at 10 mA g^{-1}. After the 1st discharge, the original peaks of Fe^{3+} and Mn^{4+} decrease and new peaks represent Fe^{2+}, Mn^{3+} and Mn^{2+} appear.[1–4] As the voltage is increased to 3.8 V in the 2nd cycle，it is evident that the Fe^{2+} and Mn^{2+} are oxidized which is in according

with the alkali ion desertion progress. When the electrode is discharged to 1.6 V in the 2nd cycle, we again find the ratio increasing of Fe^{2+} and Mn^{2+} and the ratio decreasing of Fe^{3+} and Mn^{3+}. The result presented here is a primary qualitative analysis. As in the transformation of KFM electrodes to XPS equipment, the contact to air is inevitable and it's not fit for estimating the capacity of KFM.

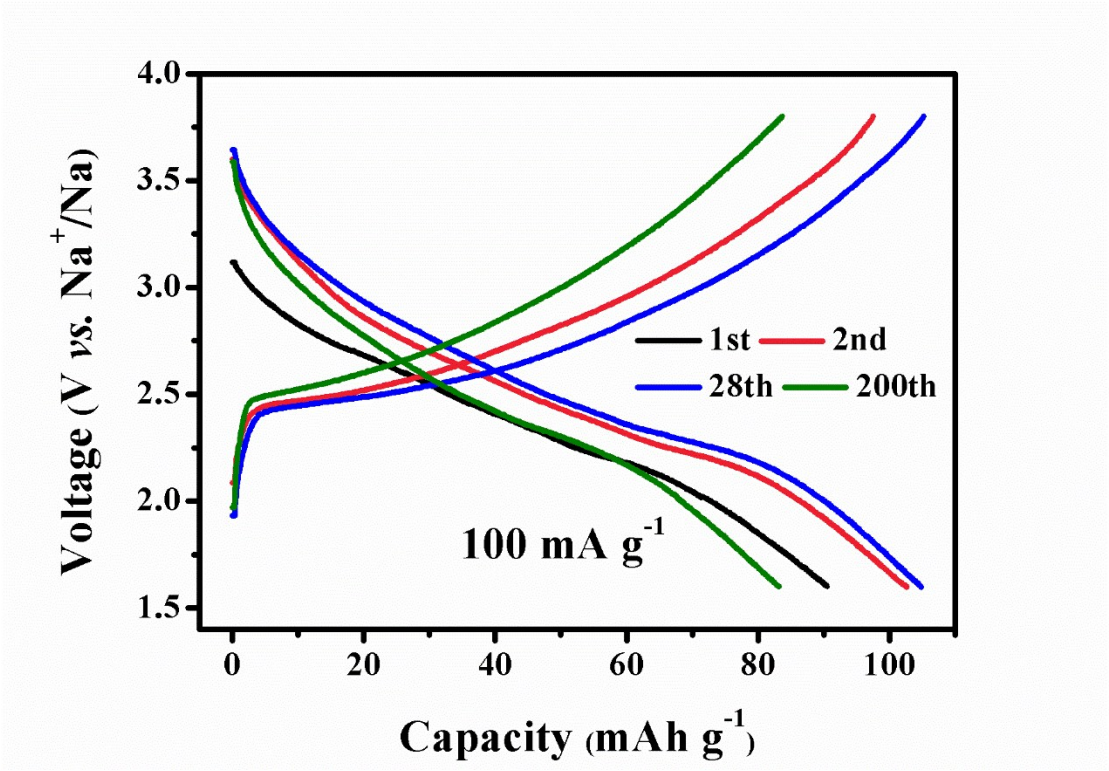

Fig. S7 Discharge/charge curves of KFM at 100 mA g^{-1}.

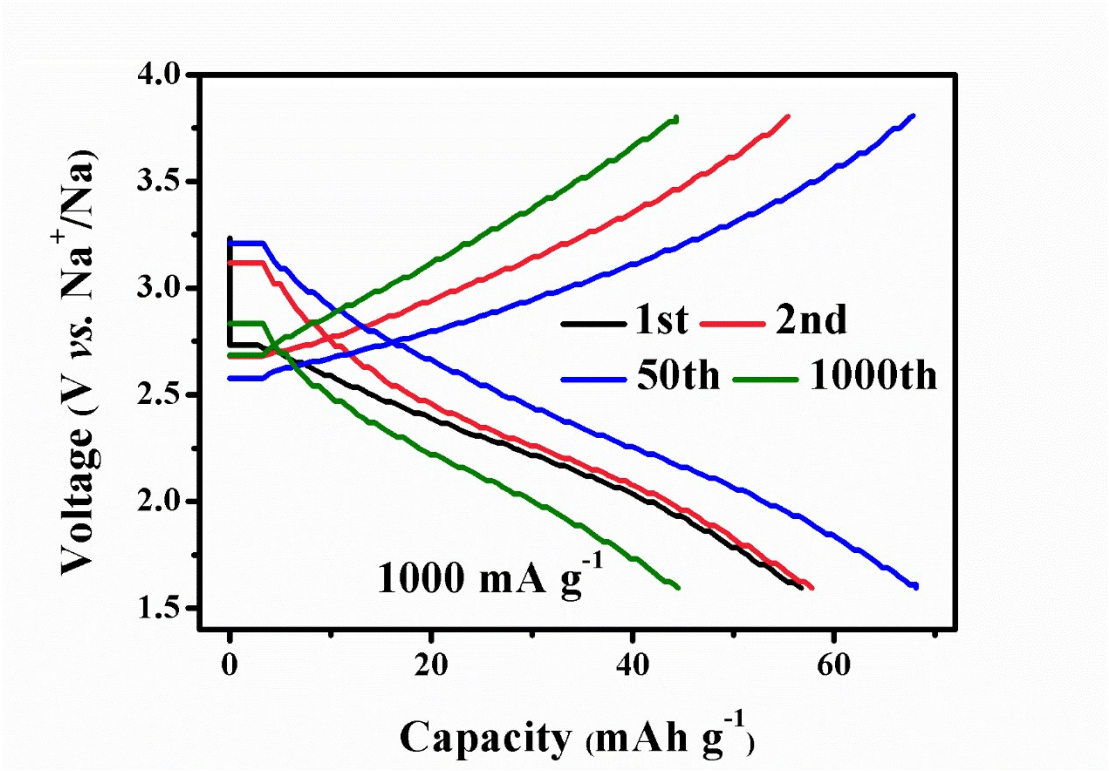

Fig. S8 Discharge/charge curves of KFM at 1000 mA g^{-1}

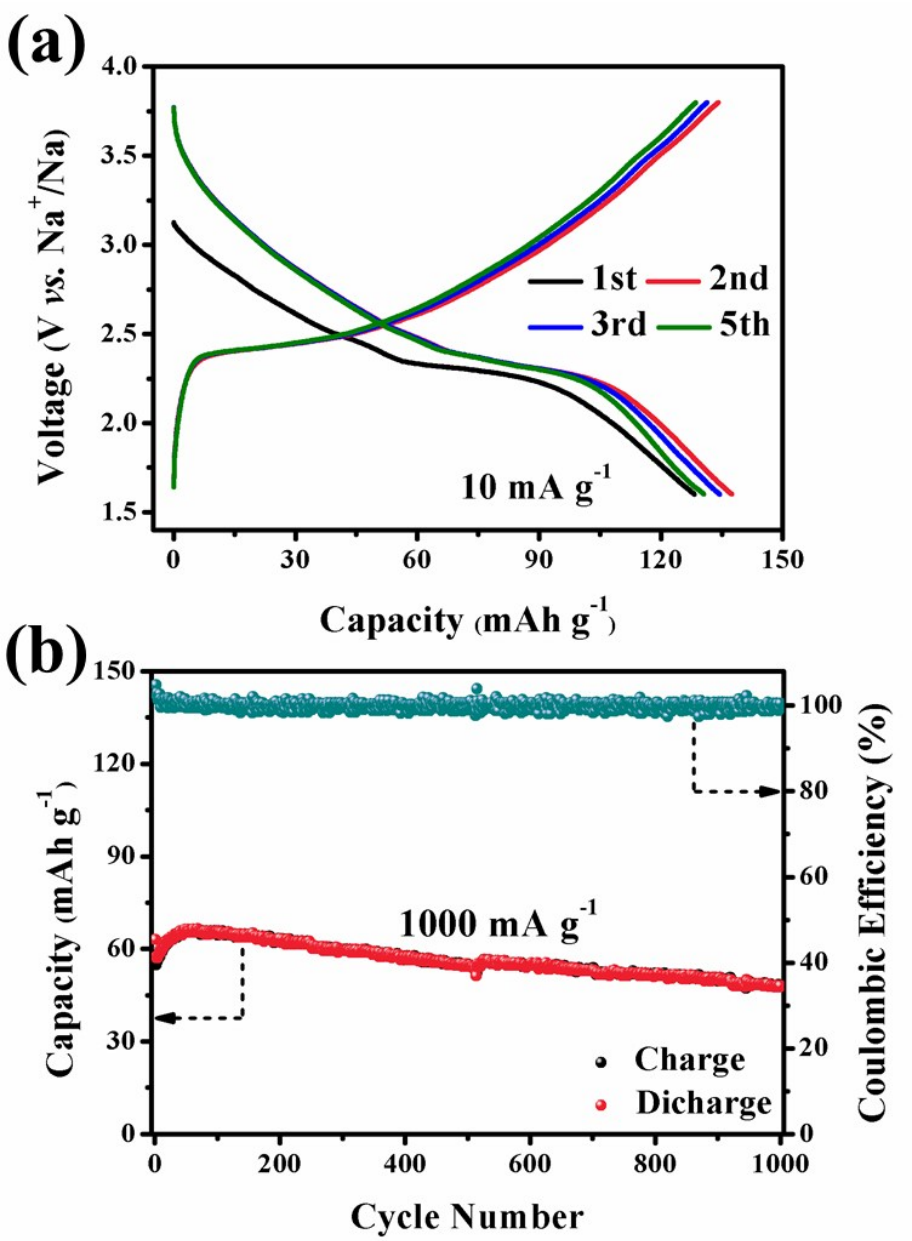

Fig. S9 (a) Discharge/charge curves of 200 °C-heated KFM at 10 mA g^{-1}. (b) The cycle performances of 200 °C heated KFM at 1000 mA g^{-1}.

The 200 °C-heated KFM shows initial discharge capacity of 128.3 mAh g^{-1} at 10 mAh g^{-1} and the discharge capacity of the 5th cycle is 130.6 mAh g^{-1} (Fig. S9a). The 200 °C heated KFM also shows considerable cycle performance at 1000 mA g^{-1} that a maximum discharge capacity of 66.5 mAh g^{-1} together with a discharge capacity of 48.0 mAh g^{-1} at the 1000th cycle are delivered (Fig. S9b).

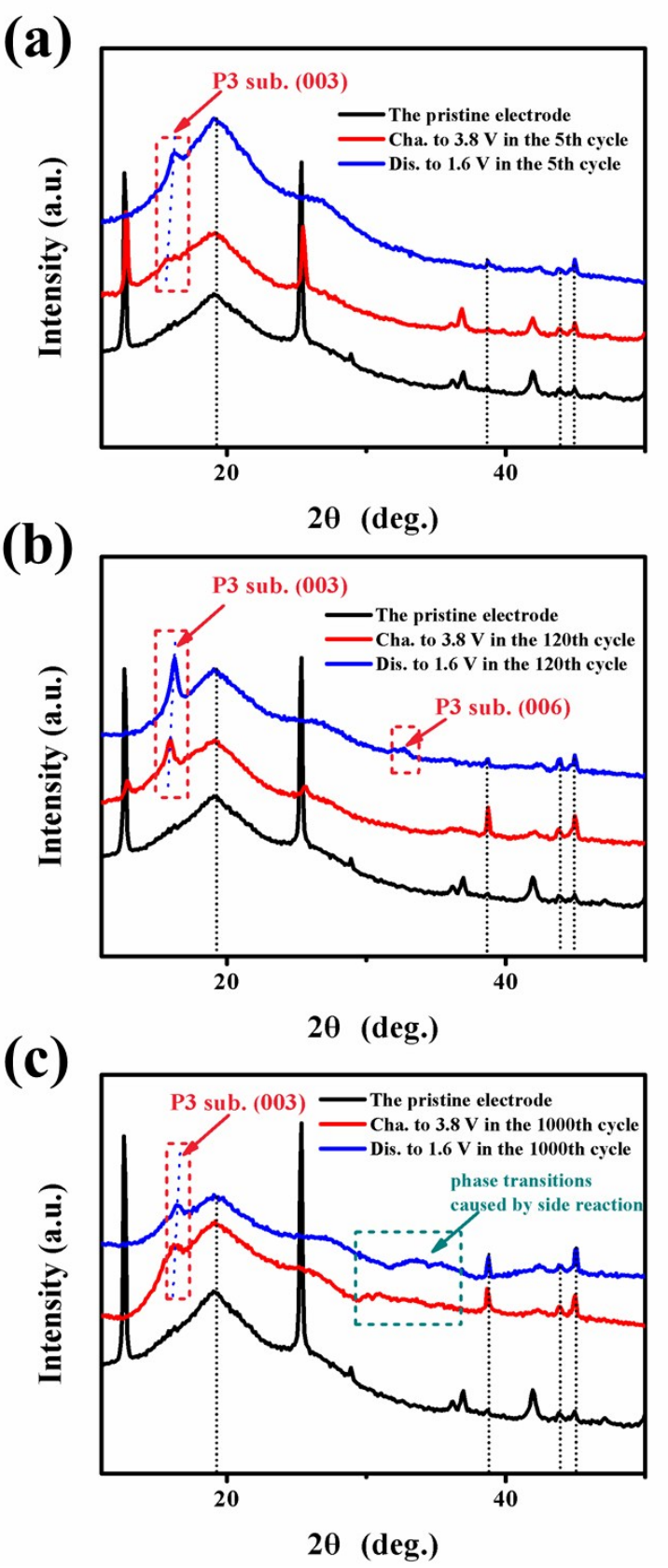

Fig. S10 (a) XRD curves of the electrodes at the end of charge/discharge of 5th, (b) 120th and (c) 1000th.

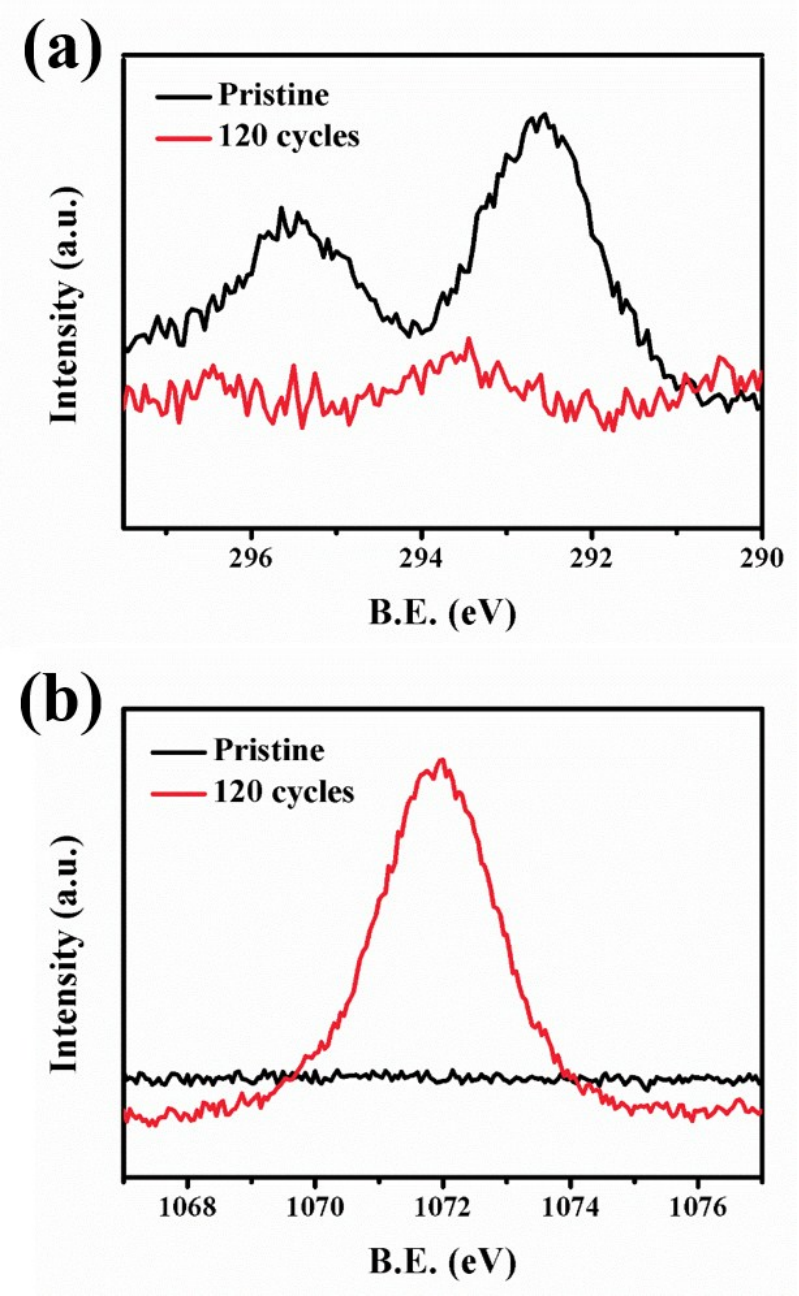

Fig. S11 (a) K and (b) Na XPS of the pristine sample and the electrode after 120 cycles.

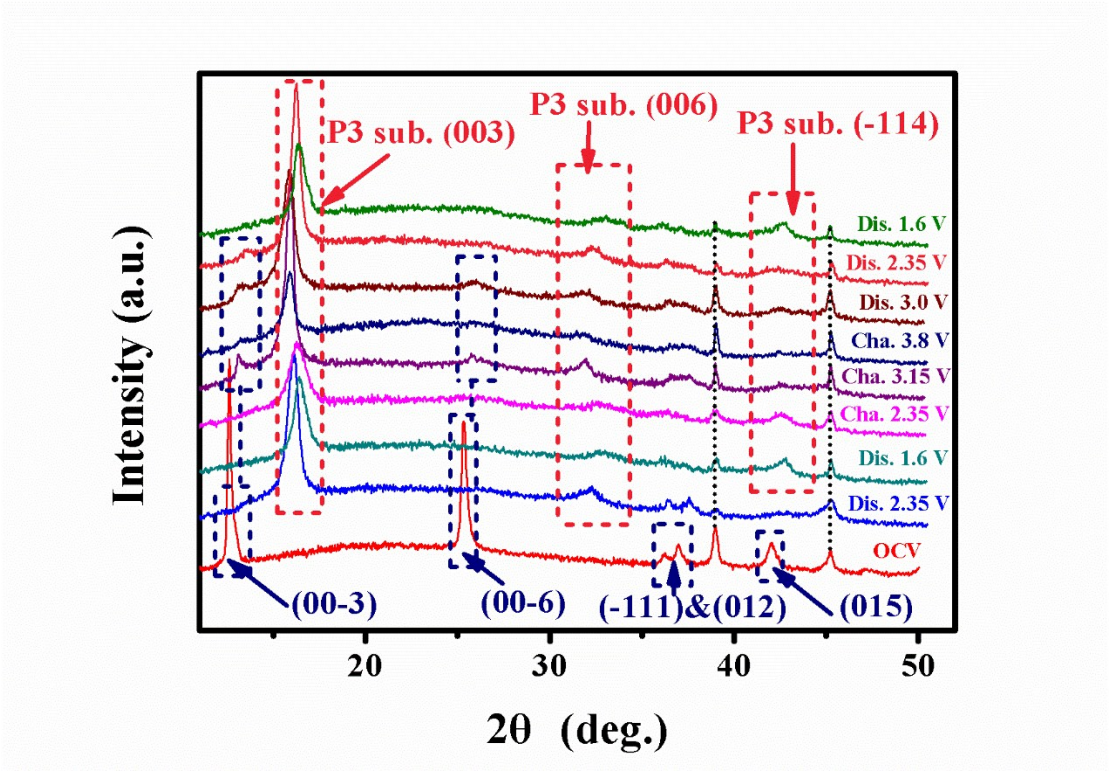

Fig. S12 The corresponding XRD patterns (without protection by Kapton films) of different stages in Fig. 5a (bottom to top—A to I), the black dashed lines marked peaks are those originated from the aluminum current collectors.

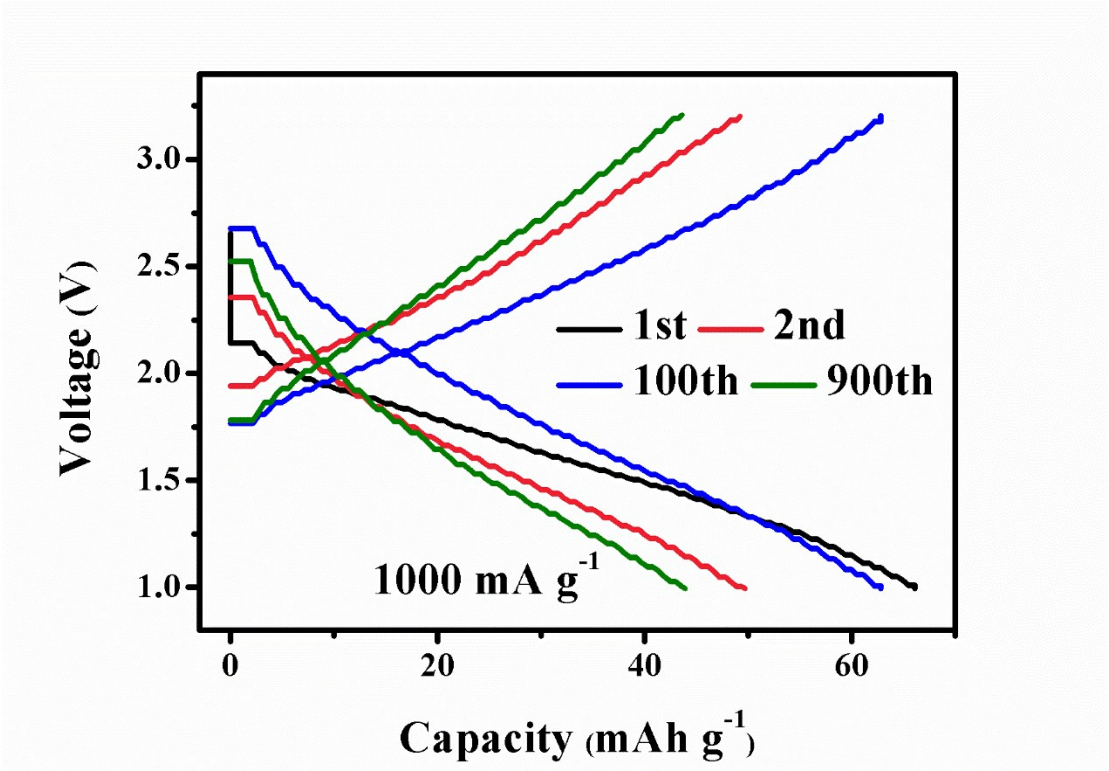

Fig. S13 Discharge/charge curves of the full battery at 1000 mA g^{-1}

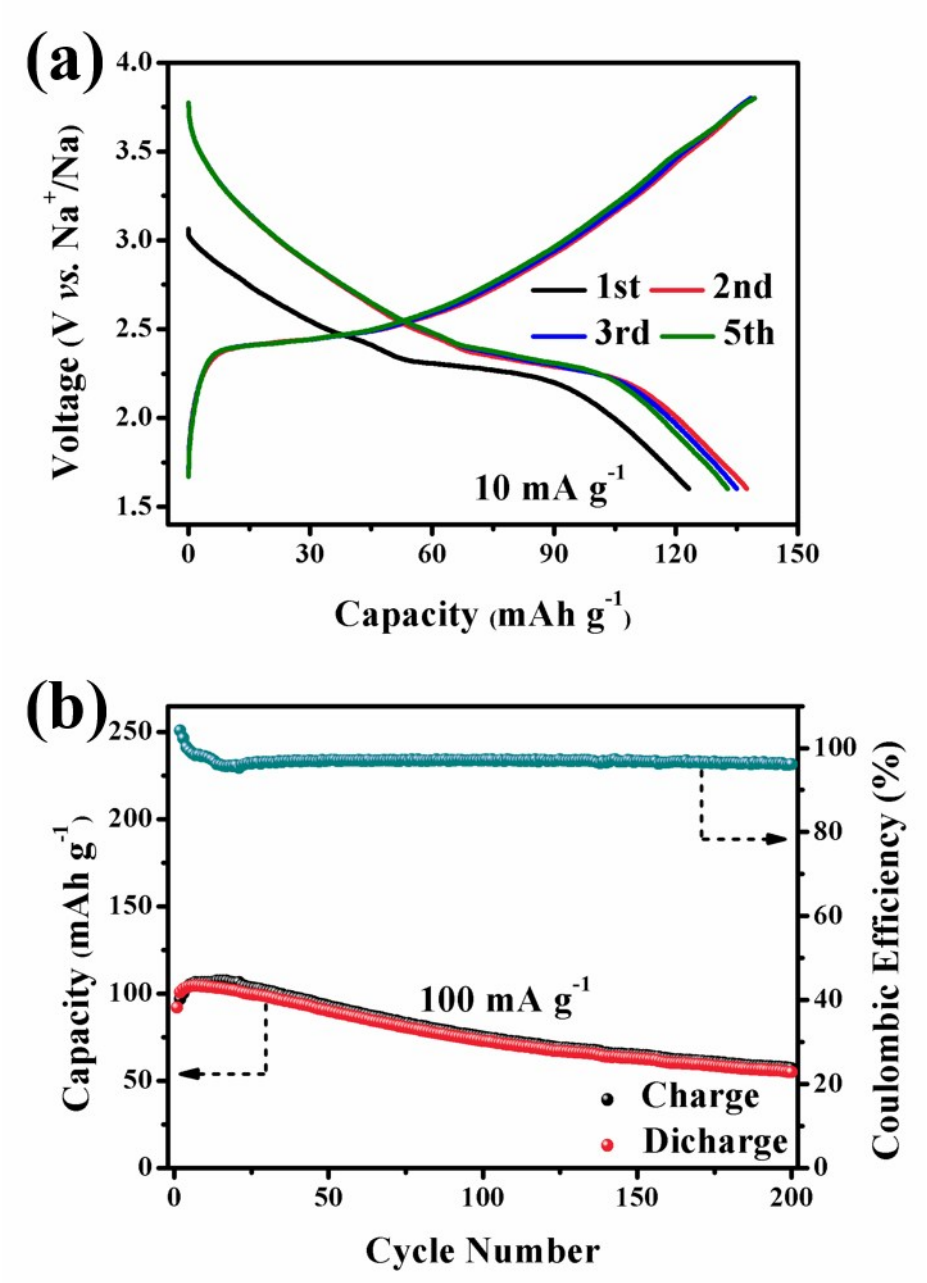

Fig. S14 (a) Discharge/charge curves of KFM at 10 mA g^{-1} in the electrolete without FEC additive. (b) The cycle performances of KFM at 100 mA g^{-1} in the electrolyte without FEC additive.

To further explore the efficacy of KFM, the electrochemical performance of the material with FEC-free electrolyte was tested for comparison (Fig. S14a, b). The

KFM demonstrates approximate initial capacities as the FEC-contained ones, but the KFM shows relative lower coulombic efficiencies both at 10 and 100 mA g^{-1} and only a discharge capacity of 55.0 mAh g^{-1} is obtained after 200 cycles at 100 mA g^{-1}.

Table S3. Summary of the typical low-cost cathodes for NIBs.

Materials	Max capacity	Cycle number/cycle rate	Full cells	Ref.
O3-Na $[Fe_{1/2}Mn_{1/2}]O_2$	100–110 mAh g^{-1}	30/12 mA g^{-1}	-	[5]
P2-Na2/3$[Fe_{1/2}Mn_{1/2}]O_2$	190 mAh g^{-1}	30/12 mA g^{-1}	-	[5]
P2-$Na_{7/9}Cu_{2/9}Fe_{1/9}Mn_{2/3}O_2$	89 mAh g^{-1}	150/100 mA g^{-1}	-	[6]
Romanechite-structured $Na_{0.31}MnO_{1.9}$	About 90 mAh g^{-1}	100/5 C charge, 0.2 C discharge	-	[7]
$FePO_4$	151 mAh g^{-1}	160/20 mA g^{-1}	-	[8]
$NaFe(SO_4)_2$	About 85 mAh g^{-1}	80/0.2C	-	[9]
This work	137.5 mAh g^{-1}	1000/1000 mA g^{-1}	220.5 Wh kg^{-1} and 4340 W kg^{-1}	-

Table S4. Summary of some representative state-of-the-art cathode materials for NIBs. (Note: The energy/power densities of full cells are all calculated based on the mass of cathode material)

Materials	Half cells max capacity	Half cell cycle number/cycle rate	Full cells energy/power densities	Full cell cycles/ Average potential	Ref.
$Na_2Co_2(SeO_3)_3$–GO	75 mAh g^{-1}	50/4.9 mA g^{-1}	-	-	[10]
$Na_{1.1}V_3O_{7.9}$@rGO	174 mAh g^{-1}	500/1000 mA g^{-1}	-	-	[11]
$NaNi_{0.45}Cu0.05Mn_{0.4}Ti_{0.1}O_2$	124 mAh g^{-1}	500/1 C	-	-	[12]
$NaVPO_4F$/C	120 mAh g^{-1}	1000/286 mAh g^{-1}	112 Wh kg^{-1}/ 200 W kg^{-1}	50/1.4 V	[13]
$Na_3V_2(PO_4)_3$	113 mAh g^{-1}	1000/10 C	134 Wh kg^{-1}/13200 W kg^{-1}	300/1.3 V	[14]
$Na[Ni0.25Fe0.5Mn_{0.25}]O_2$/C	130 mAh g^{-1}	50/0.5 C	312 Wh kg^{-1}/3120 W kg^{-1}	150/2.4 V	[15]
$K_{0.33}Co_{0.53}Mn_{0.47}O_2 \cdot 0.39H_2O$	114 mAh g^{-1}	130/500 mA g^{-1}	186.1 Wh kg^{-1} /2634 W kg^{-1}	100/2.5 V	[16]
This work	137.5 mAh g^{-1}	1000/1000 mA g^{-1}	220.5 Wh kg^{-1} /4340 W kg^{-1}	900/ 2.1 V	-

References

[1] Q. An, F. Lv, Q. Liu, C. Han, K. Zhao, J. Sheng, Q. Wei, M. Yan, L. Mai, *Nano Lett.*, 2014, **14**, 6250.

[2] L. Li , A.-R. O. Raji, J. M. Tour, *Adv. Mater.*, 2013, **25**, 6298.

[3] A. Baylet, S. Royer, C. Labrugère, H. Valencia, P. Marécot, J. M. Tatibouët, D. Duprez, *Phys. Chem. Chem. Phys.*, 2008, **10**, 5983.

[4] P. R. Chowdhury, K. G. Bhattacharyya, *RSC Adv.*, 2016, **6**, 112016.

[5] N. Yabuuchi, M. Kajiyama, J. Iwatate, H. Nishikawa, S. Hitomi, R. Okuyama, R. Usui, Y. Yamada, S. Komaba, *Nature Materials*, 2012, **11**, 512.

[6] Y. Li, Z. Yang, S. Xu, L. Mu, L. Gu, Y.-S. Hu , H. Li, L. Chen, *Adv. Sci.*, 2015, **2**, 1500031.

[7] J.-Y. Li, X.-L. Wu, X.-H. Zhang, H.-Y. Lu, G. Wang, J.-Z. Guo, F. Wan, R.-S. Wang, *Chem. Commun.*, 2015, **51**, 14848.

[8] Y. Fang, L. Xiao, J. Qian, X. Ai, H. Yang, Y. Cao, *Nano Lett.*, 2014, **14**, 3539.

[9] P. Singh, K. Shiva, H. Celio, J. B. Goodenough, *Energy Environ. Sci.*, 2015, **8** 3000.

[10] S. Y. Kim, D. Kundu, L. F. Nazar, *Adv. Energy Mater.*, 2018, **8**, 1701729.

[11] Y. Cai, F. Liu, Z. Luo, G. Fang, J. Zhou, A. Pan, S. Liang, *Energy Storage Materials*, 2018, **13**, 168.

[12] H.-R. Yao, P.-F. Wang, Y. Gong, J. Zhang, X. Yu, L. Gu, C. OuYang, Y.-X. Yin, E. Hu, X.-Q. Yang, E. Stavitski, Y.-G. Guo, L.-J. Wan, *J. Am. Chem. Soc.*, 2017, **139**, 8440.

[13] T. Jin, Y. Liu, Y. Li, K. Cao, X. Wang, L. Jiao, *Adv. Energy Mater.*, 2017, **7**, 1700087.

[14] W. Ren, Z. Zheng, C. Xu, C. Niu, Q. Wei, Q. An, K. Zhao, M. Yan, M. Qin, L. Mai, *Nano Energy*, 2016, **25**, 145.

[15] S.-M. Oh, S.-T. Myung, C. S. Yoon, J. Lu, J. Hassoun, B. Scrosati, K. Amine, Y.-K. Sun, *Nano Lett.*, 2014, **14**, 1620.

[16] S. Wang, T. Sun, S. Yuan, Y.-H. Zhu, X.-B. Zhang, J.-M. Yan, Q. Jiang, *Mater. Horiz.*, 2017, **4**, 1122.